Reproductive Sciences
2019, Vol. 26(5) 657-668

DOI: 10.1177/1933719118783881
journals.sagepub.com/home/rsx
SAGE

Hyperandrogenism Induces Histo-Architectural Changes in the Rat Uterus

Gisela Soledad Bracho, BS[1], Gabriela Anahí Altamirano, PhD[1,2], Laura Kass, PhD[1,2], Enrique Hugo Luque, PhD[1,3], and Verónica Lis Bosquiazzo, PhD[1,4]

Abstract

The effects of androgens on the uterus have been poorly studied and they need to be clarified to understand why androgen excess, such as observed in women with polycystic ovary syndrome (PCOS), is a risk factor for the development of endometrial hyperplasia, cancer, and infertility. Thus, uterine histomorphology in a PCOS experimental model was evaluated. Beginning at weaning, female rats were injected daily with dehydroepiandrosterone (DHEA, 6 mg/100 g body weight) or vehicle (sesame oil) for 20 consecutive days. On postnatal day 41 (PND41), DHEA-treated animals showed high serum testosterone levels. In addition, uterine histological analysis showed a significant increase in luminal epithelial height and glandular density without changes in cell proliferation. The thickness of the subepithelial stroma and myometrium also increased in these animals. The effect of DHEA on uterine thickness was accompanied by a significant reduction in cell density in both tissue compartments (subepithelial stroma and myometrium). Cell proliferation was not altered in the myometrium, whereas a decrease in the proliferative activity was seen at PND41 in the subepithelial stroma of DHEA animals. The analysis of the extracellular space showed that the changes in the thickness of the subepithelial stroma and myometrium were related to an increase in the organization of collagen fibers and water imbibition. The latter was associated with higher aquaporin 3 and 8 expression. This study provides evidence to further the understanding of PCOS-associated hyperandrogenism effects on uterine architecture. This could have implications for the regulation of uterine function and the development of uterine lesions.

Keywords

uterus, dehydroepiandrosterone, aquaporin, collagen, cell proliferation

Introduction

Androgen excess is one of the most common endocrine disorders of reproductive-age women. Among the disorders that result from androgen excess is polycystic ovary syndrome (PCOS), which occurs in approximately 4% to 18% of reproductive-age women worldwide.[1] The detrimental effects of excessive androgen in the endometrium lead to fertility problems[2,3] and can induce hyperplasia and endometrial cancer.[4,5] There have been limited studies in this regard, and the possible mechanisms underlying these disorders await complete elucidation.

The uterus is a hormone-dependent multicellular tissue that consists of stromal (fibroblastic and muscular) and epithelial (luminal and glandular) compartments, each with a distinct identity and role in reproductive physiology.[6] The effects of estrogens on uterine function have been extensively studied, but androgens have recently emerged as key players in the regulation of uterine function with controversial evidence. Androgens have growth- and differentiation-promoting actions in the rodent uterus.[7,8] The administration of testosterone (T) or dihydrotestosterone (DHT) to immature rats increased uterine weights.[9] Dihydrotestosterone increased endometrial and myometrial area, demonstrating the trophic effects of DHT on the adult mouse uterus.[6] Androgen receptor (AR)-knockout female mice have thinner uterine walls and reduced total uterine area compared to wild-type controls,[8] suggesting that the growth-promoting role of androgens in the uterus is mediated through

[1] Instituto de Salud y Ambiente del Litoral (ISAL UNL-CONICET), Facultad de Bioquímica y Ciencias Biológicas, Universidad Nacional del Litoral, Santa Fe, Argentina
[2] Cátedra de Patología Humana, Facultad de Bioquímica y Ciencias Biológicas, Universidad Nacional del Litoral, Santa Fe, Argentina
[3] Cátedra de Fisiología Humana, Facultad de Bioquímica y Ciencias Biológicas, Universidad Nacional del Litoral, Santa Fe, Argentina
[4] Departamento de Bioquímica Clínica y Cuantitativa, Facultad de Bioquímica y Ciencias Biológicas, Universidad Nacional del Litoral, Santa Fe, Argentina

Corresponding Author:
Verónica Lis Bosquiazzo, Instituto de Salud y Ambiente del Litoral (ISAL, UNL-CONICET), Facultad de Bioquímica y Ciencias Biológicas, Universidad Nacional del Litoral, Ciudad Universitaria, Paraje El Pozo, Casilla de Correo 242, 3000 Santa Fe, Argentina.
Email: vlbosqui@fbcb.unl.edu.ar

ARs. In contrast, other studies have demonstrated an inhibition of uterine growth and changes in the rates of cell proliferation and/or apoptosis in the uterus after androgen exposure.[10,11] This effect was reversed by an antiandrogen, indicating that this action is mediated by ARs.[10]

In the uterine stroma, the fibroblast and smooth muscle cells are interspersed with interstitial collagens. These collagens are large rigid molecules that are responsible for the mechanical strength of the uterine tissue as well as the other tissues in the body.[12-14] Estradiol (E2) administration to ovariectomized immature rats induced an extensive collagen matrix remodeling of the endometrial stroma,[15] while the endometrial stroma of androgenized rats showed an increase in the amount of organized collagen oriented parallel rather than perpendicular to the surface epithelium compared with normal rats.[16] Moreover, different studies have demonstrated that E2 and DHT have overlapping but distinct effects on genes involved in collagen matrix remodeling.[7,17]

On the other hand, the uterine stroma can also be modified by water imbibition. Water movement across cells can occur by diffusion through either the lipid bilayer or protein water channels termed aquaporins (AQPs).[18,19] Several subtypes of AQPs are also permeable to small molecules,[20] and recent evidence has demonstrated that AQPs can facilitate cell migration, invasion, and proliferation in endometrial cancer development.[21] Estradiol causes the highest AQP2 protein and messenger ribonucleic acid (mRNA) expression, whereas progesterone (P4) causes the highest AQP1, 5, and 7 protein and mRNA expression in the uterus.[22] Like P4, T induces the upregulation of *Aqp 1*, *5*, and *7* expression levels in the uterus.[23]

Despite all the abovementioned data, the effects of androgens in the uterus remain poorly studied and need to be clarified to understand why androgen excess is a risk factor for the development of endometrial hyperplasia, cancer, and infertility. In the present study, we evaluated the effects of hyperandrogenism on uterine histomorphology using a dehydroepiandrosterone (DHEA) treatment–induced PCOS rat model.

Materials and Methods

Animals

The experimental protocols were designed in accordance with the Guide for the Care and Use of Laboratory Animals issued by the US National Academy of Sciences and approved by the ethics committee of the Facultad de Bioquímica y Ciencias Biológicas, Universidad Nacional del Litoral (Santa Fe, Argentina). Rats of an inbred Wistar-derived strain at the Department of Human Physiology (Facultad de Bioquímica y Ciencias Biológicas, Universidad Nacional del Litoral) were kept in a controlled environment (22°C $\pm$ 2°C; 14 hours of light from 0600 to 2000) with free access to pellet laboratory chow (Nutrición Animal, Santa Fe, Argentina). Rats were housed in stainless steel cages with sterile pine wood shavings as bedding. Tap water was supplied ad libitum in glass bottles with rubber stoppers.

Experimental Design and Sample Collection

The hyperandrogenized environment of PCOS was reproduced in rats by the subcutaneous injection of DHEA (Sigma-Aldrich, Buenos Aires, Argentina). Female Wistar rats (21 days old) were injected daily with DHEA (DHEA group, 6 mg/100 g body weight, dissolved in 0.1 mL sesame oil, n = 9) or sesame oil (control group, n = 10) for 20 consecutive days. The animals were euthanized at postnatal day 41 (PND41) via CO_2 asphyxiation, and 2 hours before the autopsy, each rat was injected intraperitoneal (ip) with thymidine analog bromodeoxyuridine (BrdU; 60 mg/kg; Sigma-Aldrich) in order to evaluate cell proliferation. Upon autopsy, blood as well as ovarian and uterine tissues were collected and processed for different experimental purposes. Serum samples were stored at −80°C until hormone assays were performed. For histological evaluation and/or immunohistochemistry (IHC), the ovaries and one-half of 1 uterine horn of each rat were fixed in 10% (vol/vol) buffered formalin and embedded in paraffin. The other half of the uterine horn was immediately frozen in liquid nitrogen and stored at −80°C for RNA extraction followed by Reverse transcription polymerase chain reaction (RT-PCR) assays. The remaining uterine horn was weighed to evaluate water content. Taking into account that PCOS is diagnosed by 2 of the following features: (1) oligo- or anovulation, (2) clinical and/or biochemical signs of hyperandrogenism, or (3) polycystic ovaries,[24] we investigated serum T levels and ovarian histomorphology to confirm whether PCOS was induced by DHEA treatment.

Uterine Wet and Dry Weight

The uteri were excised, trimmed free of fat and any adhering nonuterine tissue, pierced, and blotted to remove excess fluid. The body of the uterus was cut just above its junction with the cervix and at the junction of the uterine horn and the ovaries. The uterus was then weighed (wet weight). The uterine dry weight was then determined by drying the uteri at a temperature of 70°C for a minimum of 24 hours in an oven before reweighing.[25] The water content was calculated as the difference between wet and dry weight.

Hormone Assay

Serum E2, T, and P4 levels were determined by chemiluminescence assays, using an Immulite 2000 system (Siemens Healthcare, Buenos Aires, SA, Argentina), following the manufacturer's specifications. The intra-assay coefficient of variation was 6.7% for E2, 10.1% for T, and 9.7% for P4. As an indirect measure of aromatase activity, the E2/T ratio was calculated.[26,27]

Ovarian and Uterine Morphology

Histology. Ovarian and uterine samples embedded in paraffin were cut into 5-µm sections, mounted on slides coated with 3-aminopropyl triethoxysilane (Sigma-Aldrich), and stained with hematoxylin and eosin for light microscopy (Olympus

BH2, Tokyo, Japan). Ovarian sections were analyzed for the presence of cystic follicles. Uterine sections were examined to determine luminal epithelial cell height, glandular density, and cell density. Three uterine sections per animal were evaluated, and at least 10 images were recorded in each section with a Spot Insight V3.5 color video camera (Diagnostic Instruments, Sterling Heights, Michigan) attached to a BH2 microscope, Olympus. The luminal epithelial cell height was measured from the apical (luminal) surface to the basement membrane, as previously described.[28] To determine the glandular density, the area occupied by the uterine glands was determined and referenced to the subepithelial stroma area using an Image-Pro Plus 4.1.0.1 system (Media Cybernetics, Silver Spring, Maryland). The cell density was defined as the ratio between the nuclear area and total stromal area (subepithelial or myometrium).[29] To quantify the area occupied by nuclei, we created an automated sequence operation using Auto-Pro macro language (Image-Pro Plus 4.1.0.1 system). Uterine glands and blood vessels cells were not included. Because the density is a dimensionless parameter, the results are expressed as arbitrary units.

Organization of collagen fibers. To analyze the organization of the collagen fibers in the uterus, the collagen birefringence of picrosirius-stained samples was quantified by polarization microscopy.[30] For each animal, 10 images were captured, digitized, and analyzed as described by Kass et al.[31] The subepithelial stroma area or myometrium area occupied by organized collagen was measured as the integrated optical density (IOD) using Image-Pro Plus 4.1.0.1 system (Media Cybernetics). The digitized images were converted to gray scale, and the IOD was calculated as a linear combination of the average gray intensity and the relative area occupied by the stroma. The results are expressed in arbitrary units.

Immunohistochemistry

Uterine sections (5 μm in thickness) were immunostained to detect the expression of vimentin, α-smooth muscle actin (α-SMA), AQP 3-7-8, AR, estrogen receptor α (ESR1), and BrdU-positive cells (proliferative index). Immunoperoxidase staining was performed as previously described.[32] Primary antibodies (Table 1) were incubated overnight at 4°C. The reactions were developed using a streptavidin–biotin peroxidase method and diaminobenzidine (Sigma-Aldrich). Samples were mounted with permanent mounting medium (Eukitt; Sigma-Aldrich). Each IHC run included negative controls in which the primary antibody was replaced by nonimmune goat serum (Sigma-Aldrich). To test the specificity of the antibodies against AQP3 and AQP8, the primary antibodies were preabsorbed with the antigenic peptides as indicated by the manufacturer (Alomone Lab, Jerusalem, Israel). Then, the antibody–antigen complexes were applied in the immunohistochemical assays. In the negative controls, the primary antibody was replaced with nonimmune rabbit serum.

Table 1. Antibodies Used for Immunohistochemistry.

Antibodies	Dilution	Supplier
Primary antibodies		
Antivimentin (clone v9)	1/200	Novocastra, Newcastle upon Tyne, United Kingdom.
Anti-smooth muscle α- actin (α-SMA clone α-SMA-1)	1/200	Novocastra, Newcastle upon Tyne, United Kingdom.
Anti-ESR1 (clone 6F-11)	1/200	Novocastra, Newcastle upon Tyne, United Kingdom.
Anti-AR	1/400	Santa Cruz Biotechnology Inc (Santa Cruz, California).
Anti-BrdU (clone 85-2c8)	1/100	Novocastra, Newcastle upon Tyne, United Kingdom.
Anti-AQP3	1/300	Alomone Labs, Jerusalem, Israel.
Anti-AQP7	1/100	Alpha Diagnostic International, San Antonio, Texas.
Anti-AQP8	1/25	Alomone Labs, Jerusalem, Israel.
Secondary antibodies		
Anti-mouse	1/80	Sigma-Aldrich (Buenos Aires, Argentina)
Anti-rabbit	1/200	Sigma-Aldrich (Buenos Aires, Argentina)

Abbreviations: AQP, aquaporin; AR, androgen receptor; BrdU, bromodeoxyuridine; ESR1, estrogen receptor α.

Thickness of the subepithelial stroma and myometrium. The thickness of the subepithelial stroma and myometrium was determined on uterine sections stained with antivimentin and anti-α-SMA, respectively. Three sections per animal were analyzed by using an Image-Pro Plus system (Media Cybernetics) as previously described.[33]

Cell proliferation. The incorporation of BrdU in the S phase of the cell cycle was quantitatively analyzed on immunostained tissue sections. Proliferative indices were obtained as a percentage of positive cells by counting 2000 cells/tissue section of luminal and glandular epithelium. These measurements were performed by 2 trained observers who were blinded to the animal's treatment. In the subepithelial stroma and myometrium, the percentage of cell proliferation was determined by using an Image-Pro Plus analyzer system (Media Cybernetics). At least 10 images of each area were evaluated through color segmentation analysis, which extracts objects by locating all objects of a specific color (blue or brown stain).

Steroid hormone receptors. To measure the IOD of ESR1 immunostaining in the subepithelial stroma and myometrium, at least 10 fields were recorded in each section, and 3 sections per animal were evaluated and analyzed using an Image-Pro Plus

Table 2. Primers and PCR Products for Real-Time Quantitative Polymerase chain reaction (PCR).

Genes	Sense Primer	Antisense Primer	Product Size (bp)
AQP1	5′-CATTGGCTTGTCTGTGGCTC-3′	5′-CCCACCCAGAAAATCCAGTG-3′	132
AQP2	5′-GGACCTGGCTGTCAATGCTC-3′	5′-GTCGGTGGAGGCAAAGATGC-3′	109
AQP3	5′-CTGTGGTTCCGTGGCTCAAG-3′	5′-AGCAGGGTTCAAGTGGGCTC-3′	139
AQP4	5′-GAGCCAGCATGAATCCAGC-3′	5′-AGGCTTCCTTTAGGCGACG-3′	171
AQP5	5′-CTCCCCAGCCTTATCCATTG-3′	5′-GAAAGATCGGGCTGGGTTCA-3′	94
AQP6	5′-CTGCGGTCATTGTTGGGAAG-3′	5′-CGGTCTTGGTGTCAGGAAAC-3′	117
AQP7	5′-GTGCTACAGAAGACTTGGGTGC-3′	5′-TAGCTGCCAAGCCTTTCTCC-3′	119
AQP8	5′-CTGTGTGTATGGGTGCCGTC-3′	5′-AGGCACGAGCAGGGTTCATG-3′	132
AQP9	5′-AGGACGGTGCCAAGAAGAGC-3′	5′-GGACCGCTTGGGCAATAGAG-3′	132
L19	5′-AGCCTGTGACTGTCCATTCC-3′	5′-TGGCAGTACCCTTCCTCTTC-3′	99

Abbreviation: AQP, aquaporin.

system (Media Cybernetics) as previously described.[34] The IOD was measured as a linear combination between the average gray intensity and the relative area occupied by positive cells. Because the IOD is a dimensionless parameter, the results are expressed as arbitrary units.

Reverse Transcription and Real-Time Quantitative PCR Analysis

RNA extraction and reverse transcription. Individual uterine horn samples were homogenized in TRIzol (Invitrogen, Carlsbad, California), and RNA was prepared according to the manufacturer's protocol. The concentration of total RNA was assessed by A260, and the samples were stored at −80°C until needed. Equal quantities (1 μg) of total RNA were reverse-transcribed into copy desoxiribonucleic acid (cDNA) with Moloney Murine Leukemia Virus Reverse Transcriptase (10 units; Promega, Madison, Wisconsin) as previously described.[32]

Real-time quantitative PCR. Each reverse-transcribed product was diluted with ribonuclease-free water to a final volume of 60 μL and further amplified in triplicate using the real-time Rotor-Gene Q (Qiagen Tecnolab, Buenos Aires, Argentina). An optimized real-time PCR protocol was used to analyze the mRNA expression levels of total *Aqp1* to *Aqp9* and *L19*. Ribosomal protein L19 mRNA was selected as a housekeeping gene (internal control) since the expression of L19 mRNA remained constant in all experimental conditions. The primer sequences designed for cDNA amplification are described in Table 2. For cDNA amplification, 5 mL of cDNA was combined with HOT FIREPol Eva Green qPCR Mix Plus (Solis BioDyne, Biocientífica, Rosario, Argentina) and 10 pmol of each primer (Invitrogen) in a final volume of 20 mL. Product purity was confirmed by dissociation curves, and random samples were subjected to agarose gel electrophoresis. Controls containing no template DNA were included in all assays and yielded no consistent amplification. The relative expression levels of each target were calculated based on the cycle threshold (CT) method.[35] The CT for each sample was calculated using the Rotor-Gene Q ePure Detection software (version 1.7; Qiagen Tecnolab) with an automatic fluorescence threshold (Rn) setting. *L19* was used to normalize the CT values of the genes evaluated. The relative expression levels of each target were calculated using the standard curve method.[36]

Statistical Analysis

All data are expressed as the mean ± standard error of the mean (SEM). Mann-Whitney *U* tests were used to compare the experimental and control groups (SPSS-PASW Statistics v. 18). Correlations were performed using the Spearman analysis (SPSS-PASW Statistics v. 18). $P < .05$ was considered statistically significant.

Results

Polycystic Ovary Syndrome and Endocrine Profile

On PND41, the T levels were significantly increased in animals that received DHEA injections compared to animals that received vehicle injections (Figure 1A). No significant differences in E2 and P4 serum levels were observed between experimental groups (E2: control 62.45 ± 9.75 pg/mL vs DHEA 66.22 ± 1.85 pg/mL; P4: control 9.30 ± 1.83 ng/mL vs DHEA 6.96 ± 2.34 ng/mL). Animals treated with DHEA had significantly lower values of E2/T ratio compared to the control group (E2/T ratio: control 344.2 ± 18.24 vs DHEA 126 ± 34.88). The ovaries of control animals showed follicles at different stages of development, which is indicative of normal ovarian morphology, whereas ovaries from the rats in the DHEA group exhibited a swollen appearance with multiple cystic follicles (Figure 1B and C).

Effects of PCOS-Related Androgen Excess on Uterine Histomorphology

To elucidate the actions of hyperandrogenism on the uterus, both horn uteri were removed, and during visual inspection, we observed larger and opaquer uteri in DHEA animals compared with control animals (Figure 2A). Uterine histological analysis showed significant increases in the epithelial height and glandular density that were not associated with changes in cell proliferation (Figure 2B-G).

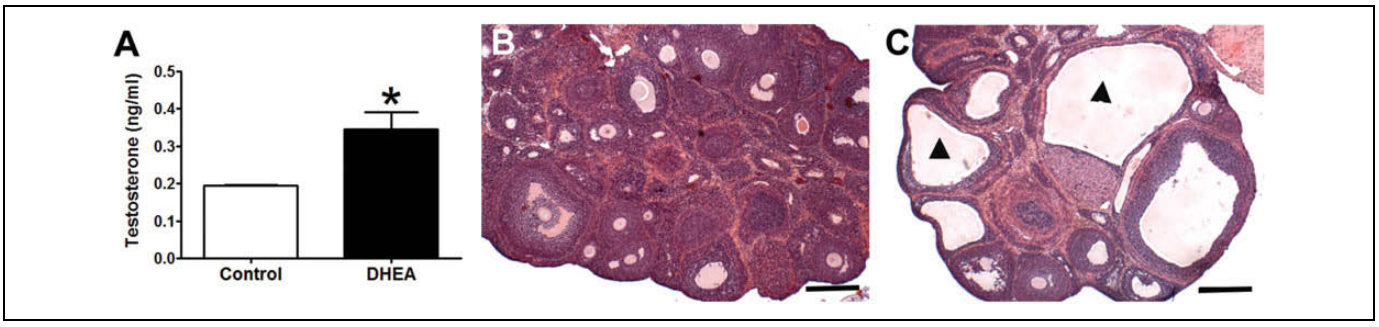

Figure 1. Serum testosterone levels and ovarian histology of control and DHEA-treated rats at PND41. (A) The bar graph shows the serum levels of testosterone. Each column represents the mean ± standard error of mean (SEM) of 9 to 10 animals/group. Asterisks denote $P < .05$. Representative photomicrographs of ovaries stained with hematoxylin and eosin from control (B) and DHEA (C) animals. Arrowhead indicates cystic follicle formation. Scale bar: 200 μm. DHEA indicates dehydroepiandrosterone; PND41, postnatal day 41.

The subepithelial stroma and myometrium thickness increased in rats treated with DHEA (Figure 2B, C, H, and K). To determine whether these changes were associated with changes in the number of cells and/or size of the extracellular space, we evaluated the uterine cell density, cell proliferation, organization of collagen fibers, and water imbibition. The increase in uterine thickness was accompanied by a significant reduction in cell density in both the subepithelial stroma and myometrium (Figure 2I-L). Negative correlations were found between thickness and cell density in both uterine compartments (subepithelial stroma: $r = -0.6236$, $P = .0009$; myometrium: $r = -0.7620$, $P = .0004$). Then, we studied whether the alterations in cell density may be due to changes in cell proliferation. In the myometrium, BrdU incorporation showed no differences between groups, whereas in the subepithelial stroma, the proliferative activity in animals treated with DHEA decreased (Figure 2J and M). Cell density and cell proliferation showed a positive correlation in this last region ($r = 0.7407$, $P = .0024$).

Next, we evaluated whether extracellular space was modified. In DHEA animals, the organization of collagen fibers was higher than in control animals, both in the subepithelial stroma and myometrium (Figure 3). The water content was also increased in DHEA-treated rats (control 9.42 ± 1.87 mg/cm vs DHEA 24.49 ± 1.39 mg/cm). Regarding *Aqps* expression, except for *Aqp6*, *Aqp1* to *9* were detected at the mRNA level in rat uterine tissues (Figure 4). *Aqp1, 2, 4, 5,* and *9* mRNA levels did not show differences between experimental groups (Figure 4). The DHEA treatment increased the expression levels of *Aqp3* and *8* mRNA but decreased the expression levels of *Aqp7* mRNA compared to those of control rats (Figure 4). Figure 5 shows representative images of the IHC assays performed to determine the location of the AQPs in the uterine tissue. In the uterine epithelial cells, AQP3 was found in the cytoplasm in the control group; however, its expression was both cytoplasmic and nuclear in DHEA animals (Figure 5B and C). In the subepithelial stroma and myometrium, AQP3 was expressed in the cell nucleus in both experimental groups (Figure 5B, C, and D-F). Aquaporin 7 was localized in the cytoplasm of the uterine epithelial cells in both control and DHEA groups (Figure 5H, I, K, and L). Aquaporin 8 showed a cytoplasmic localization in the uterine epithelial and subepithelial stromal cells in both groups (Figure 5N and O); in DHEA, AQP8 was induced in the cytoplasm of myometrial cells (Figure 5Q and R).

Effects of PCOS-Related Androgen Excess on Expression of Androgen and ESRs

Considering that steroid hormones' regulation of functional uterine differentiation is through binding to their receptors, we studied whether the hyperandrogenized environment of PCOS affects AR and ESR1 expression. Figure 6 shows representative photomicrographs of AR immunodetection from the uterus of control or DHEA-treated rats. The AR expression was induced in all cellular compartments after DHEA treatment. In the luminal and glandular epithelium, the protein was localized in the cytoplasm, whereas in the subepithelial stroma and myometrium, the immunostaining was nuclear. The ESR1 expression did not change between experimental groups (data not shown).

Discussion

The uterus is a hormone-dependent multicellular tissue. Unlike estrogen and P4, which have been extensively studied, androgens have recently emerged as key players in the regulation of uterus function. This is mainly due to the effects observed in the uteri of women with PCOS. Polycystic ovary syndrome is associated with infertility and a significantly higher risk of endometrial hyperplasia and cancer.[37] In the present study, the hyperandrogenized environment of PCOS was reproduced in rats by injections of DHEA using a well-characterized model that shows the salient features of women with PCOS.[38-40] Here, rats treated with DHEA presented higher serum levels of androgens and abnormal ovarian morphology.

Androgens promote the growth and differentiation of the rodent uterus.[7] Uteri from rats treated with DHEA (aromatizable androgen) show significant changes in uterine weight and increases in the uterine diameter and epithelial cell height

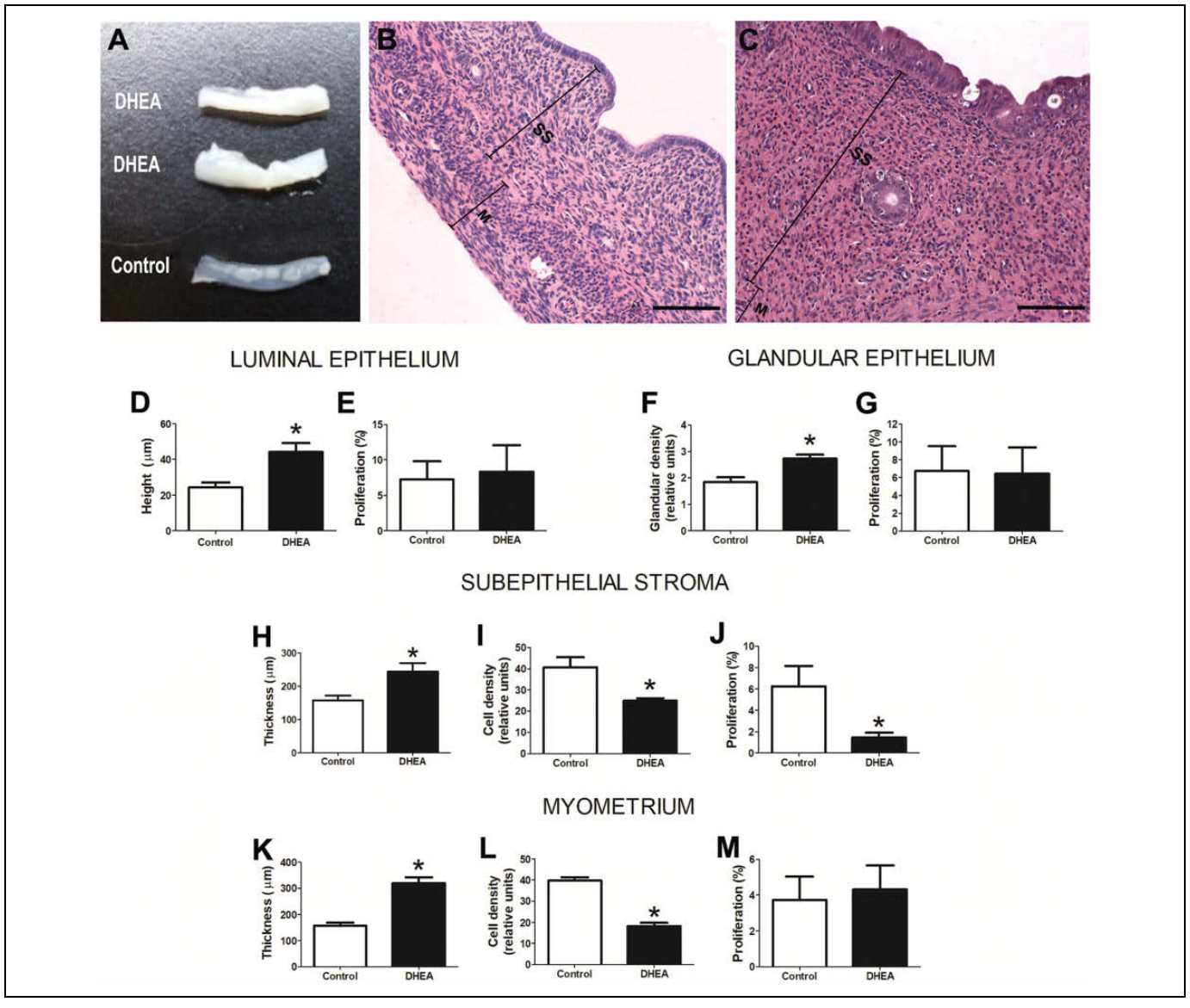

Figure 2. Effects of PCOS-related androgen excess on rat uterine histology at PND41. (A) Photographs of representative uteri collected from control and DHEA-treated animals. Uterine sections stained with hematoxylin and eosin from control (B) and DHEA-treated (C) animals. Scale bar: 100 μm. Quantification of height (D) and cell proliferation (E) of the luminal epithelium; glandular density (F); glandular proliferation (G); thickness, cell density, and proliferation of the subepithelial stroma (H-J); and thickness, cell density, and proliferation of the myometrium (K-M). Each column represents the mean ± SEM of 9 to 10 animals/group. Asterisks denote $P < .05$. DHEA indicates dehydroepiandrosterone; M, myometrium; PCOS, polycystic ovary syndrome; PND41, postnatal day 41; SS, subepithelial stroma.

compared with control animals.[38,39,41] When rats were treated with DHT (nonaromatizable androgen) or the synthetic androgen mibolerone, an increase in endometrial and myometrial areas accompanied by a significant decrease in cell density was observed.[6,7] In agreement with these results, we demonstrated that treatment with DHEA also resulted in an increased thickness and reduced cell density in both cellular compartments. In addition, we showed that AR expression was induced after DHEA treatment. Previous studies have demonstrated that AR-knockout animals and rats treated with an antiandrogen show significant reductions in uterine diameter and total uterine area, indicating that a disruption in AR signaling leads to abnormal uterine development.[8,42] The abovementioned findings and our present results show that parameters of uterine histology, such as surface area and cell density, were modified by both nonaromatizable and aromatizable androgens, suggesting that these are androgenic effects that would be mediated by ARs.

The reduced uterine cell density observed in DHEA animals could be explained by changes in the number of cells or in the size of the intercellular space, induced by such features as collagen organization and/or water imbibition. Simitsidellis et al[6] detected very low cell proliferation in the uterine stroma of control and DHT-treated rats. In another experiment, early

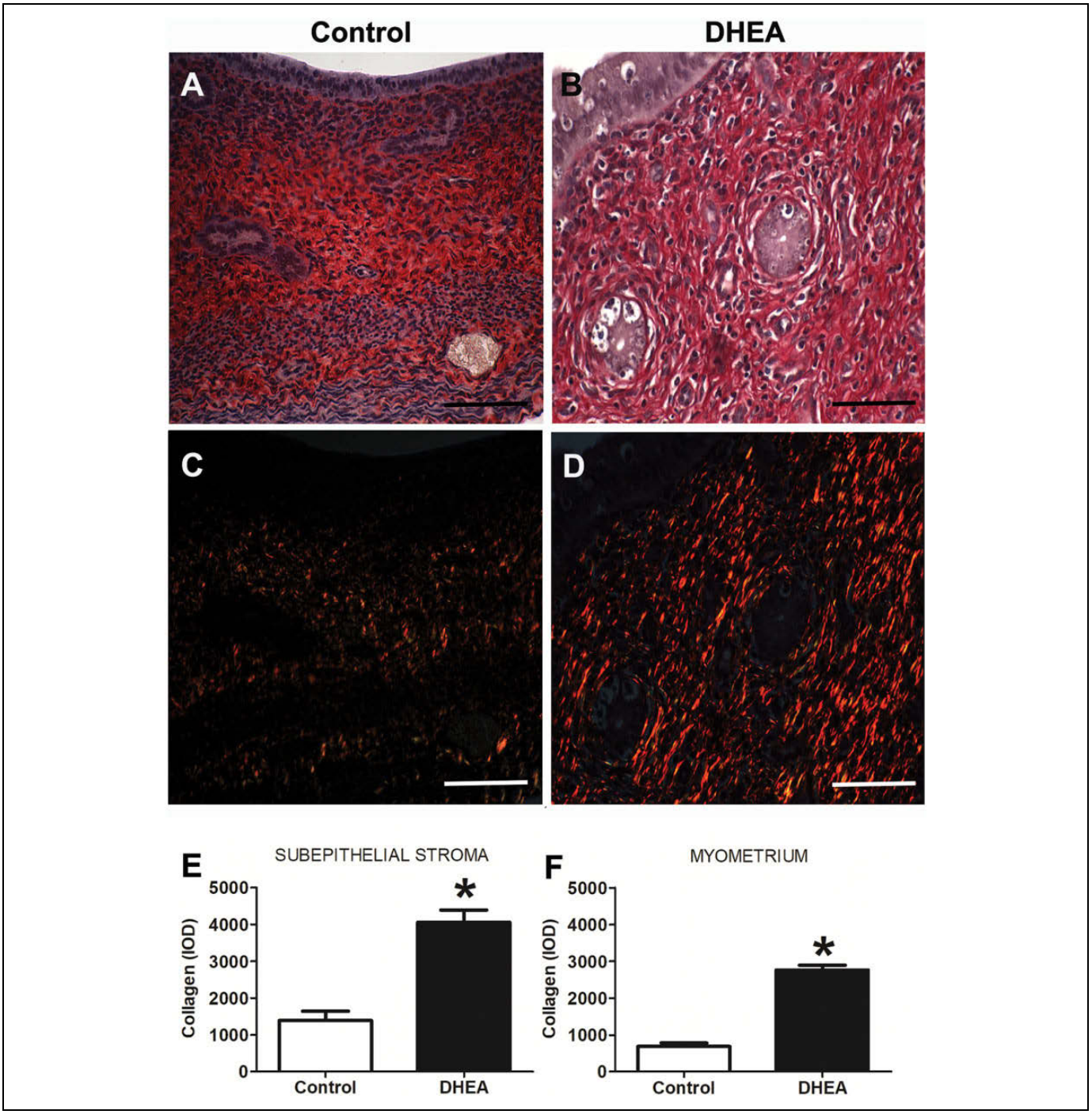

Figure 3. Effects of PCOS-related androgen excess on rat uterine organization of collagen fibers at PND41. Uterine sections were studied by the picrosirius-polarization method (a procedure specific for the detection of collagenous structures in tissue sections). All brightly birefringent structures, which shine against a dark background, are of a collagenous nature. The sections were studied under conventional illumination (A and B) and polarization microscopy (C and D) in the same field. Scale bar: 50 μm. E and F, Quantification of organized collagen fibers in the subepithelial stroma and myometrium. Each column represents the mean ± SEM of 9 to 10 animals/group. Asterisks denote $P < .05$. PCOS indicates polycystic ovary syndrome; PND41, postnatal day 41.

androgen exposure affected the uterine cellular machinery regulating proliferation in the adult, which demonstrated decreased proliferation indices in the myometrium.[11] Here, we demonstrated that DHEA treatment modified proliferative activity in the rat uterus. We observed a decrease in cell proliferation in the uterine stromal cells that could explain, at least in part, the reduced cell density observed in this compartment.

Regarding the changes in the intercellular space, Sourla et al[43] demonstrated that in ovariectomized adult animals

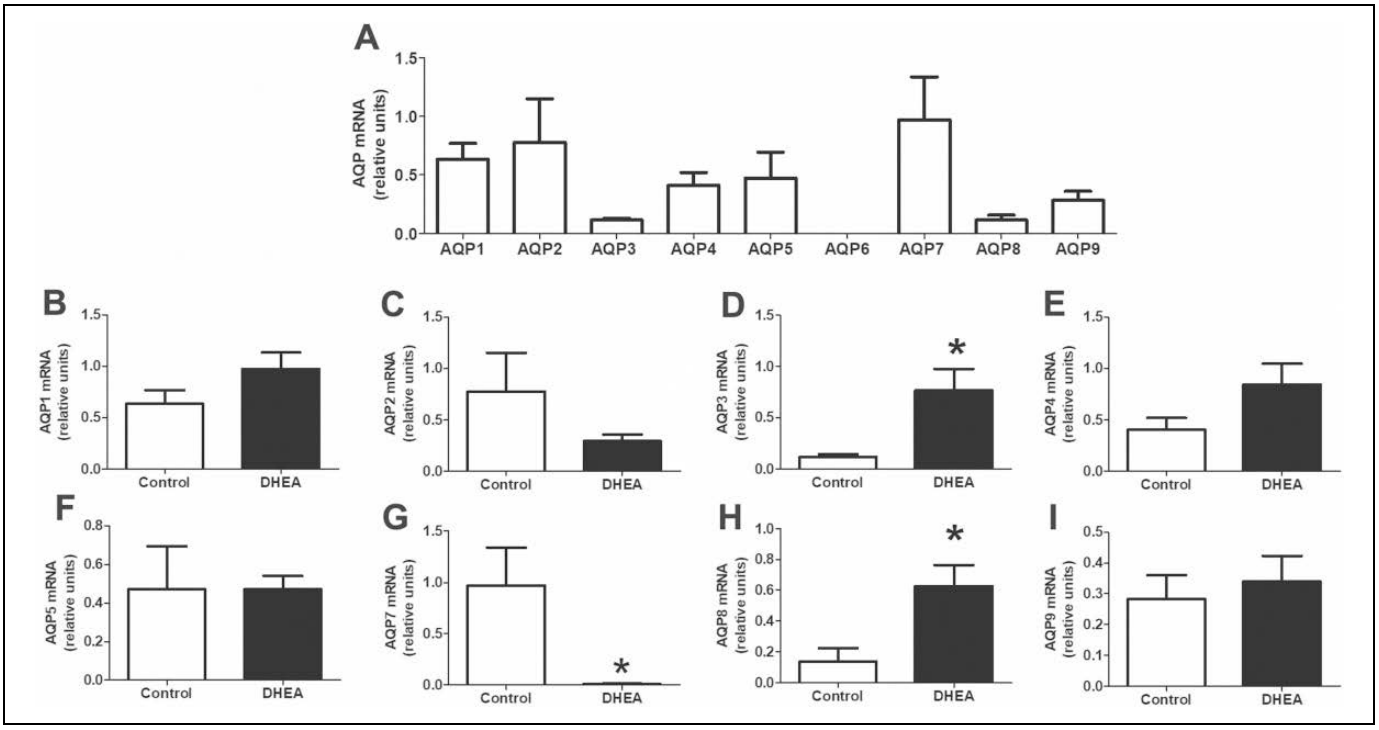

Figure 4. Effects of PCOS-related androgen excess on rat uterine *Aqps* mRNA expression at PND41. (A) Quantification of *Aqps* transcripts detected in the control group. (B) *Aqp1*, (C) *Aqp2*, (D) *Aqp3*, (E) *Aqp4*, (F) *Aqp5*, (G) *Aqp7*, (H) *Aqp8*, and (I) *Aqp9* expression in control and DHEA groups. Each column represents the mean ± SEM of 9 to 10 animals/group. Asterisks denote $P < .05$. AQP indicates aquaporin; DHEA, dehydroepiandrosterone; PCOS, polycystic ovary syndrome; PND41, postnatal day 41.

treated with DHEA, a partial reversal of the uterine atrophy seen in untreated animals was observed. This effect was characterized by an increased thickness of the myometrium primarily and, to a lesser extent, the endometrial layer and was principally related to an increase in the amount of collagen in the stroma.[43] Previously, Lobl and Maenza[16] demonstrated that the endometrial stroma of androgenized rats showed an increase in the amount of organized collagen compared with the normal rat. Here, we demonstrated that there was a higher level of organization of collagen fibers in both the subepithelial stroma and myometrium of PCOS rats, which is supporting evidence that the extracellular matrix was also modified. The extent of collagen abundance and its organization into thick linearized bundles have been correlated with tumor aggression.[44] The importance of collagen cross-linking and stiffening with malignant transformations was illustrated through in vivo studies that showed that premalignant mammary epithelial cells transplanted into mouse mammary glands whose collagen cross-linking had been enhanced transformed into invasive, rapidly growing tumors.[45,46] Considering that women with PCOS have a high risk of developing endometrial hyperplasia and uterine cancer, the greater organization of collagen in DHEA group animals could contribute to and be a predisposing factor for the development of these conditions. More experiments are necessary to clarify this issue.

Aquaporins are expressed and regulated by steroid hormones in the uterus, where they appear to mediate water imbibition and the movement of water and other molecules (ie, urea and glycerol NH3). Salleh et al[23] showed that the levels of *Aqp1* mRNA were elevated in rats receiving estrogen, and the levels of *Aqp1*, *5*, and *7* mRNA were increased in rats receiving T treatment, where the T effects were antagonized by an antiandrogen (flutamide). Another study showed that AQP1, 3, and 8 are constitutively expressed in the ovariectomized mouse uterus.[18] Here, we showed that with exception of *Aqp6*, *Aqp1* to *Aqp9* mRNAs were expressed in the rat uterus, and *Aqp3* and *Aqp8* were increased in the DHEA group. These AQPs exhibited different localization patterns in the uterine tissue. Aquaporin 3 exhibited nuclear expression in all tissue compartment in DHEA animals, whereas AQP8 was expressed in the cytoplasm of the epithelial and subepithelial stromal cells in both groups. Aquaporin 8 was also induced in the myometrium of the DHEA animals. In a mouse model, the expression of AQP-3 was primarily localized in the cytoplasm of luminal epithelial cells of the uterus with scattered immunolocalization in the glandular epithelial cells and the myometrium, and AQP-8 expression was observed in the cytoplasm of stromal cells of the endometrium and the myometrium.[18] Discrepancies between these results and ours may be attributable to different animal species and experimental models. The nuclear expression pattern of AQP3 was observed in hepatocellular carcinoma[47] and has been shown to regulate gene expression.[48,49] Our results suggest that AQP3 and AQP8 could be involved in the higher water imbibition observed in the uterus of DHEA

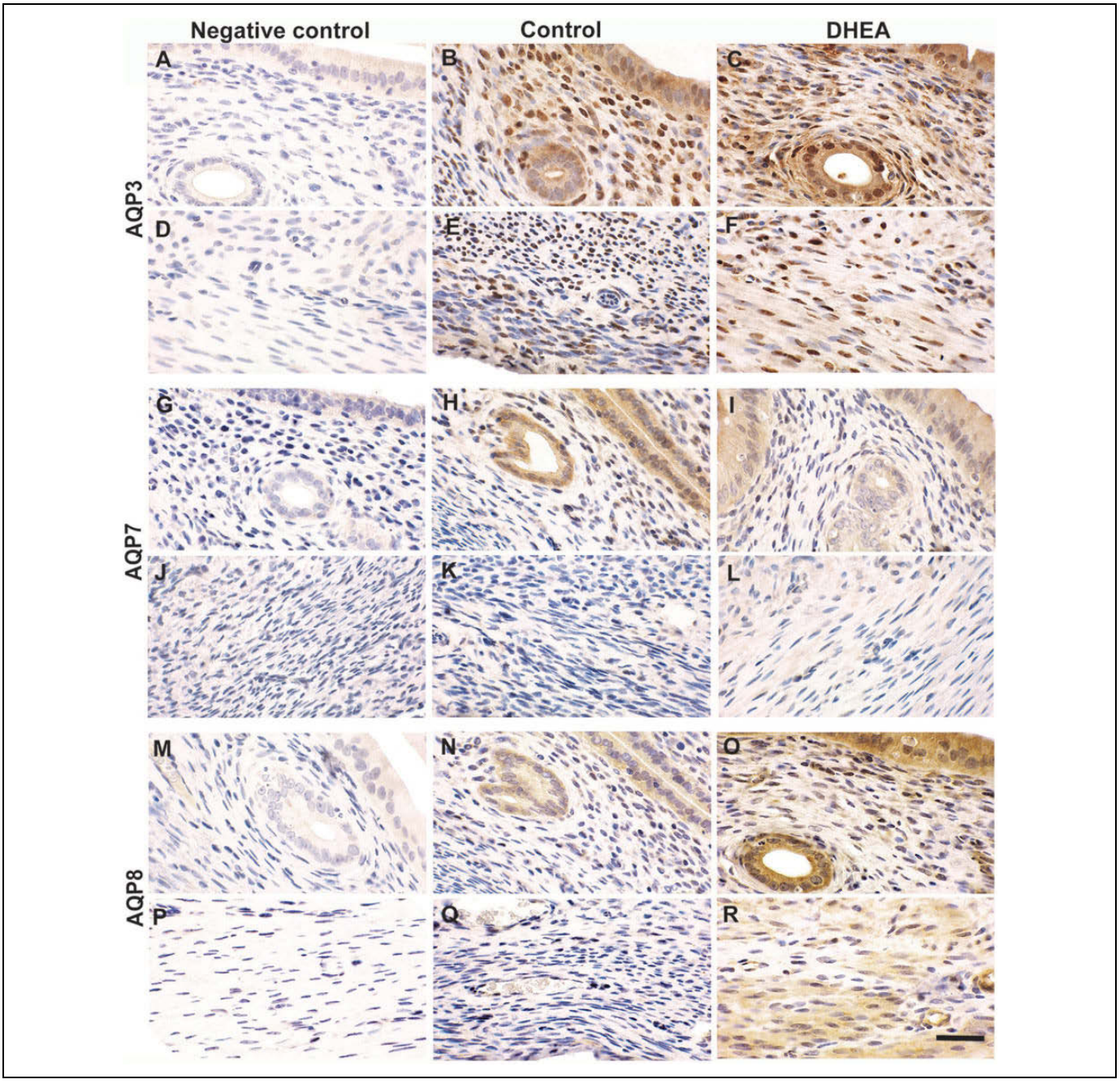

Figure 5. Effects of PCOS-related androgen excess on rat uterine AQP expression at PND41. Photomicrographs show uterine sections immunostained for AQP3 (B and C), AQP7 (H and I), and AQP8 (N and O) in the epithelial and subepithelial stromal cells, and for AQP3 (D-F), AQP7 (K and L), and AQP8 (Q and R) in the myometrial cells, both in control and DHEA groups. Primary antibodies were preabsorbed with peptides used as immunogens for AQP3 (A and D) and AQP8 (M and P). Negative control of immunohistochemistry assay replacing the primary antiserum with nonimmune rabbit serum (G and J). All these images were obtained from sections with hematoxylin counterstaining. Scale bar = 50 μm. AQP indicates aquaporin; DHEA, dehydroepiandrosterone; PCOS, polycystic ovary syndrome; PND41, postnatal day 41.

animals. Previous studies have suggested that several members of the AQP family are involved in peri-implantation fluid homeostasis. Aquaporins 3, 4, 5, and 8 help to maintain cervical water balance during pregnancy and parturition.[50] Moreover, high expression levels of AQPs are detectable in cervical carcinomas and endometriosis.[20,21,51] The inhibition of AQP2 expression in human endometrial carcinomas significantly attenuated the migration, adhesion, and invasion of endometrial carcinoma cells.[20] These antecedents provide evidence that AQPs not only modulate water or molecule movement but could also participate in tumor growth.

Together, our results suggest that the hyperandrogenized rat uterus had a greater thickness due to changes in cell proliferation, collagen organization, and water imbibition, providing

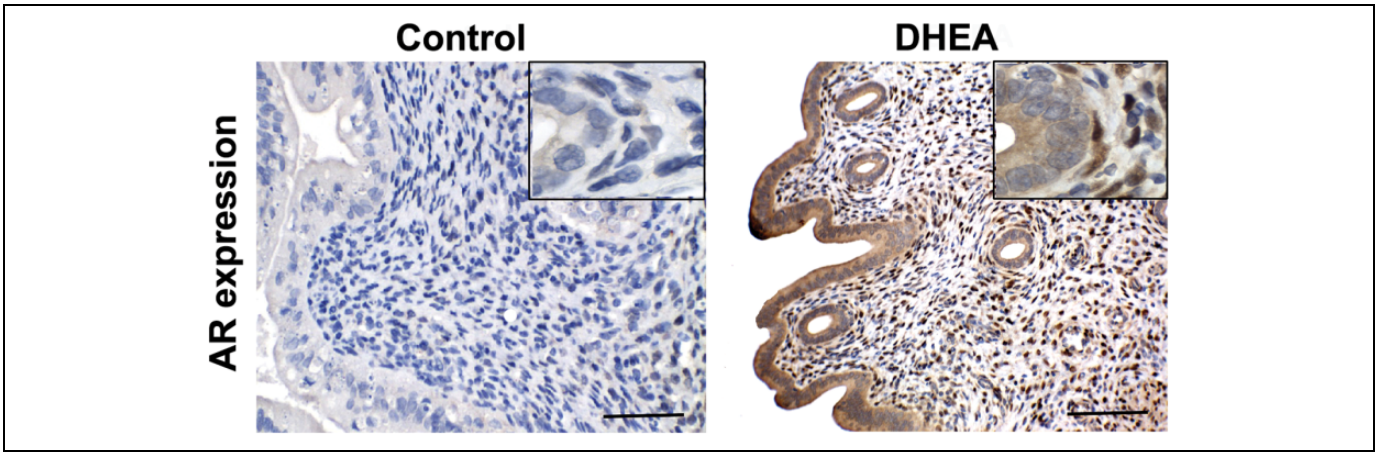

Figure 6. Effects of PCOS-related androgen excess on AR expression in the rat uterus at PND41. Representative photomicrographs of uterine sections immunostained for AR from the control (A) and DHEA-treated (B) animals. Scale bar: 100 μm. The insets show higher magnification AR-specific staining. AR indicates androgen receptor; DHEA, dehydroepiandrosterone; PCOS, polycystic ovary syndrome; PND41, postnatal day 41.

evidence for the understanding of the effects of androgens on uterine architecture and their possible association with higher risk of developing uterine pathologies in women with PCOS. We do not rule out that both DHEA itself and androgens produced by PCOS may mediate some of its actions through conversion to estrogen and affect the ER signaling pathway. However, in this study, E2 levels did not show significant differences between experimental groups and the E2/T ratio was decreased in DHEA-treated animals (suggesting that aromatase activity was not increased). Moreover, no changes in ESR1 expression were observed between groups. It remains to be established whether local estrogen (indirect) or elevated levels of androgens (direct) are responsible for the uterine phenotype described in the present study.

Authors' Note

E.H.L. and V.L.B. shared last authorship.

Acknowledgments

The authors would like to thank Dr Marinelli for his generous gift of antibodies (AQP7 and AQP8) and the Alomone Labs for its antibodies samples (AQP3 and AQP8). In addition, the authors would like to thank Juan Grant and Juan C. Villarreal, Carla Waigandt, and Dr Lucía Vigezzi (UNL) for their technical assistance and animal care. G.S.B.is a fellow of ANPCyT, G.A.A. is a fellow, and L.K., E.H.L., and V.L.B. are career investigators of CONICET.

Declaration of Conflicting Interests

The author(s) declared no potential conflicts of interest with respect to the research, authorship, and/or publication of this article.

Funding

The author(s) disclosed receipt of the following financial support for the research, authorship, and/or publication of this article: This work was supported by grants from the following: Agencia Nacional de Promoción Científica y Tecnológica (ANPCyT, PICT 2014 N°2348, N°1628, PICT 2016 N°0390), Consejo Nacional de Investigaciones Científicas y Técnicas (CONICET, PIP 00397), and Universidad Nacional del Litoral (UNL, CAID 2016 PIC 50420150100088LI). These funding sources were not involved in the study design; the collection, analysis or interpretation of the data; the writing of the report; or the decision to submit the article for publication.

References

1. Li X, Guo YR, Lin JF, Feng Y, Billig H, Shao R. Combination of Diane-35 and metformin to treat early endometrial carcinoma in PCOS women with insulin resistance. *J Cancer*. 2014;5(3):173-181.
2. Okon MA, Laird SM, Tuckerman EM, Li TC. Serum androgen levels in women who have recurrent miscarriages and their correlation with markers of endometrial function. *Fertil Steril*. 1998; 69(4):682-690.
3. Xita N, Georgiou I, Tsatsoulis A. The genetic basis of polycystic ovary syndrome. *Eur J Endocrinol*. 2002;147(6):717-725.
4. Balen A. Polycystic ovary syndrome and cancer. *Hum Reprod Update*. 2001;7(6):522-525.
5. Pillay OC, Te Fong LF, Crow JC, et al. The association between polycystic ovaries and endometrial cancer. *Hum Reprod*. 2006; 21(4):924-929.
6. Simitsidellis I, Gibson DA, Cousins FL, Esnal-Zufiaurre A, Saunders PT. A role for androgens in epithelial proliferation and formation of glands in the mouse uterus. *Endocrinology*. 2016; 157(5):2116-2128.
7. Nantermet PV, Masarachia P, Gentile MA, et al. Androgenic induction of growth and differentiation in the rodent uterus involves the modulation of estrogen-regulated genetic pathways. *Endocrinology*. 2005;146(2):564-578.
8. Walters KA, McTavish KJ, Seneviratne MG, et al. Subfertile female androgen receptor knockout mice exhibit defects in neuroendocrine signaling, intraovarian function, and uterine development but not uterine function. *Endocrinology*. 2009;150(7): 3274-3282.
9. Schmidt WN, Katzenellenbogen BS. Androgen-uterine interactions: an assessment of androgen interaction with the testosterone-

and estrogen-receptor systems and stimulation of uterine growth and progesterone-receptor synthesis. *Mol Cell Endocrinol*. 1979; 15(2):91-108.
10. Tuckerman EM, Okon MA, Li T, Laird SM. Do androgens have a direct effect on endometrial function? An in vitro study. *Fertil Steril*. 2000;74(4):771-779.
11. Guerra MT, Sanabria M, Grossman G, Petrusz P, Kempinas Wde G. Excess androgen during perinatal life alters steroid receptor expression, apoptosis, and cell proliferation in the uteri of the offspring. *Reprod Toxicol*. 2013;40:1-7.
12. Luque EH, Muñoz de Toro MM, Ramos JG, Rodriguez HA, Sherwood OD. Role of relaxin and estrogen in the control of eosinophilic invasion and collagen remodeling in rat cervical tissue at term. *Biol Reprod*. 1998;59(4):795-800.
13. Rodriguez HA, Kass L, Varayoud J, et al. Collagen remodelling in the guinea-pig uterine cervix at term is associated with a decrease in progesterone receptor expression. *Mol Hum Reprod*. 2003; 9(12):807-813.
14. Leppert PC, Jayes FL, Segars JH. The extracellular matrix contributes to mechanotransduction in uterine fibroids. *Obstet Gynecol Int*. 2014;2014:783289.
15. Russo LA, Peano BJ, Trivedi SP, et al. Regulated expression of matrix metalloproteinases, inflammatory mediators, and endometrial matrix remodeling by 17beta-estradiol in the immature rat uterus. *Reprod Biol Endocrinol*. 2009;7:124.
16. Lobl RT, Maenza RM. Androgenization: alterations in uterine growth and morphology. *Biol Reprod*. 1975;13(3):255-268.
17. Page-McCaw A, Ewald AJ, Werb Z. Matrix metalloproteinases and the regulation of tissue remodelling. *Nat Rev Mol Cell Biol*. 2007;8(3):221-233.
18. Jablonski EM, McConnell NA, Hughes FM Jr., Huet-Hudson YM. Estrogen regulation of aquaporins in the mouse uterus: potential roles in uterine water movement. *Biol Reprod*. 2003; 69(5):1481-1487.
19. Lindsay LA, Murphy CR. Aquaporins are upregulated in glandular epithelium at the time of implantation in the rat. *J Mol Histol*. 2007;38(1):87-95.
20. Zhu C, Jiang Z, Bazer FW, Johnson GA, Burghardt RC, Wu G. Aquaporins in the female reproductive system of mammals. *Front Biosci (Landmark Ed)*. 2015;20:838-871.
21. Zou LB, Zhang RJ, Tan YJ, et al. Identification of estrogen response element in the aquaporin-2 gene that mediates estrogen-induced cell migration and invasion in human endometrial carcinoma. *J Clin Endocrinol Metab*. 2011;96(9): E1399-E1408.
22. Chinigarzadeh A, Muniandy S, Salleh N. Estradiol, progesterone and genistein differentially regulate levels of aquaporin (AQP)-1, 2, 5 and 7 expression in the uteri of ovariectomized, sex-steroid deficient rats. *Steroids*. 2016;115:47-55.
23. Salleh N, Mokhtar HM, Kassim NM, Giribabu N. Testosterone induces increase in aquaporin (AQP)-1, 5, and 7 expressions in the uteri of ovariectomized rats. *J Membr Biol*. 2015;248(6): 1097-1105.
24. Rosenfield RL. The polycystic ovary morphology-polycystic ovary syndrome spectrum. *J Pediatr Adolesc Gynecol*. 2015; 28(6):412-419.
25. Ashby J, Odum J, Foster JR. Activity of raloxifene in immature and ovariectomized rat uterotrophic assays. *Regul Toxicol Pharmacol*. 1997;25(3):226-231.
26. Horng SG, Wang TH, Wang HS. Estradiol-to-testosterone ratio is associated with response to metformin treatment in women with clomiphene citrate-resistant polycystic ovary syndrome (PCOS). *Chang Gung Med J*. 2008;31(5):477-483.
27. Chen J, Shen S, Tan Y, et al. The correlation of aromatase activity and obesity in women with or without polycystic ovary syndrome. *J Ovarian Res*. 2015;8:11.
28. Varayoud J, Monje L, Bernhardt T, Muñoz-de-Toro M, Luque EH, Ramos JG. Endosulfan modulates estrogen-dependent genes like a non-uterotrophic dose of 17beta-estradiol. *Reprod Toxicol*. 2008;26(2):138-145.
29. Durando M, Kass L, Piva J, et al. Prenatal bisphenol A exposure induces preneoplastic lesions in the mammary gland in Wistar rats. *Environ Health Perspect*. 2007;115(1):80-86.
30. Montes GS. Structural biology of the fibres of the collagenous and elastic systems. *Cell Biol Int*. 1996;20(1):15-27.
31. Kass L, Ramos JG, Ortega HH, et al. Relaxin has a minor role in rat mammary gland growth and differentiation during pregnancy. *Endocrine*. 2001;15(3):263-269.
32. Bosquiazzo VL, Vigezzi L, Muñoz-de-Toro M, Luque EH. Perinatal exposure to diethylstilbestrol alters the functional differentiation of the adult rat uterus. *J Steroid Biochem Mol Biol*. 2013; 138:1-9.
33. Guerrero Schimpf M, Milesi MM, Ingaramo PI, Luque EH, Varayoud J. Neonatal exposure to a glyphosate based herbicide alters the development of the rat uterus. *Toxicology*. 2017;376:2-14.
34. Ramos JG, Varayoud J, Bosquiazzo VL, Luque EH, Muñoz-de-Toro M. Cellular turnover in the rat uterine cervix and its relationship to estrogen and progesterone receptor dynamics. *Biol Reprod*. 2002;67(3):735-742.
35. Higuchi R, Fockler C, Dollinger G, Watson R. Kinetic PCR analysis: real-time monitoring of DNA amplification reactions. *Biotechnology (N Y)*. 1993;11(9):1026-1030.
36. Cikos S, Bukovska A, Koppel J. Relative quantification of mRNA: comparison of methods currently used for real-time PCR data analysis. *BMC Mol Biol*. 2007;8:113.
37. Giudice LC. Endometrium in PCOS: Implantation and predisposition to endocrine CA. *Best Pract Res Clin Endocrinol Metab*. 2006;20(2):235-244.
38. Liu W, Liu W, Fu Y, Wang Y, Zhang Y. Bak Foong pills combined with metformin in the treatment of a polycystic ovarian syndrome rat model. *Oncol Lett*. 2015;10(3):1819-1825.
39. Lee MJ, Jang M, Bae CS, et al. Effects of oriental medicine Kyung-Ok-Ko on uterine abnormality in hyperandrogenized rats. *Rejuvenation Res*. 2016;19(6):456-466.
40. Luchetti CG, Solano ME, Sander V, et al. Effects of dehydroepiandrosterone on ovarian cystogenesis and immune function. *J Reprod Immunol*. 2004;64(1-2):59-74.
41. Kreimann EL, Cabrini RL. Subcellular redistribution of NHERF1 in response to dehydroepiandrosterone (DHEA) administration in endometrial glands of Wistar rats. *Reprod Sci*. 2013;20(1): 103-111.

42. Choi JP, Zheng Y, Skulte KA, Handelsman DJ, Simanainen U. Development and characterization of uterine glandular epithelium specific androgen receptor knockout mouse model. *Biol Reprod*. 2015;93(5):120.
43. Sourla A, Flamand M, Belanger A, Labrie F. Effect of dehydroepiandrosterone on vaginal and uterine histomorphology in the rat. *J Steroid Biochem Mol Biol*. 1998;66(3):137-149.
44. Northey JJ, Przybyla L, Weaver VM. Tissue force programs cell fate and tumor aggression. *Cancer Discov*. 2017;7(11): 1224-1237.
45. Kass L, Erler JT, Dembo M, Weaver VM. Mammary epithelial cell: influence of extracellular matrix composition and organization during development and tumorigenesis. *Int J Biochem Cell Biol*. 2007;39(11):1987-1994.
46. Levental KR, Yu H, Kass L, et al. Matrix crosslinking forces tumor progression by enhancing integrin signaling. *Cell*. 2009; 139(5):891-906.
47. Chen XF, Li CF, Lu L, Mei ZC. Expression and clinical significance of aquaglyceroporins in human hepatocellular carcinoma. *Mol Med Rep*. 2016;13(6):5283-5289.
48. Xie H, Liu F, Liu L, et al. Protective role of AQP3 in UVA-induced NHSFs apoptosis via Bcl2 up-regulation. *Arch Dermatol Res*. 2013;305(5):397-406.
49. Trigueros-Motos L, Perez-Torras S, Casado FJ, Molina-Arcas M, Pastor-Anglada M. Aquaporin 3 (AQP3) participates in the cytotoxic response to nucleoside-derived drugs. *BMC Cancer*. 2012; 12:434.
50. Anderson J, Brown N, Mahendroo MS, Reese J. Utilization of different aquaporin water channels in the mouse cervix during pregnancy and parturition and in models of preterm and delayed cervical ripening. *Endocrinology*. 2006;147(1):130-140.
51. Pan H, Sun CC, Zhou CY, Huang HF. Expression of aquaporin-1 in normal, hyperplasic, and carcinomatous endometria. *Int J Gynaecol Obstet*. 2008;101(3):239-244.